## **CONFERENCE PRE-PRINT**

# DESIGN OF THE ELECTRON CYCLOTRON HEATING EXPANSION SYSTEM ON EAST

W.Y. Xu, L.Y. Zhang, D.J. Wu, H.D. Xu, Y. Yang, J. Wang, T. Zhang, W.S. He, Y.Z. Hou Institute of Plasma Physics, Chinese Academy of Sciences Hefei, China

Email: xuweiye@ipp.cas.cn, zhangly@ipp.cas.cn, djwu@ipp.cas.cn, xhd@ipp.cas.cn

## Abstract

Electron Cyclotron Resonance Heating (ECRH) expansion system on EAST is in development. This expansion system includes two gyrotron systems. It will enhance the total ECRH's power output capability at the 140 GHz frequency to 4.5 MW for up to 1000 seconds. To accommodate the entire operational range of EAST's toroidal field, the expansion system, i.e., #5 and #6 systems, will primarily operate at 140 GHz but can switch to a secondary frequency of 105 GHz to adapt to EAST's low toroidal field operations. The dual-frequency transmission lines, antenna, and the independent control system for the #5 and #6 systems were designed. A new central timing controller was designed with three operating modes: system self-check mode, test mode, and EAST experiment mode. In test mode and EAST experiment mode, the automatic restart function can be enabled, allowing the gyrotron to restart automatically in the event of a fault interruption.

## 1. INTRODUCTION

In the research of magnetically confined fusion, Electron Cyclotron Resonance Heating (ECRH) is an efficient and highly advantageous method for plasma heating. It serves as a critical heating system for achieving high-parameter and high-confinement plasma discharges in the EAST tokamak[1].

The Phase I long-pulse high-power electron cyclotron resonance heating (ECRH) system has been developed on EAST [2]. This system consists of four sets of gyrotrons. After years of development and optimization, it has achieved an operational capability of 3.2 MW for 100–1000 seconds during EAST experiments, providing a crucial heating method for EAST's high-parameter long-pulse operation[3].

To further enhance EAST's plasma parameters, the electron cyclotron wave power needs to be increased to over 4.5 MW. Therefore, plans are underway for a Phase II ECRH upgrade for EAST.

# 2. OVERALL SYSTEM ENGINEERING DESIGN

The EAST Electron Cyclotron Resonance Heating (ECRH) system operates at a frequency of 140 GHz or 105 GHz, utilizing plasma heating by the X2 mode, with currently four subsystems [2,4,5]. We plan to upgrade the four ECRH systems to six, enhancing ECRH's power output capability at the 140 GHz frequency to 4.5 MW for up to 1000 seconds. To accommodate the entire operational range of EAST's toroidal field, the two additional systems, i.e., #5 and #6 systems, will primarily operate at 140 GHz but can switch to a secondary frequency of 105 GHz to adapt to EAST's low toroidal field operations. The layout diagram of the ECH expansion system is shown in the red rectangular area in Fig. 1.

The expanded ECRH system consists of two subsystems: #5 system and #6 system. Similar to the Phase I ECRH system, each subsystem includes the gyrotron system, the high-voltage power supply system, the transmission line and antenna system, the control and protection system, and the active cooling (water-cooling and oil-cooling) system. Each gyrotron system includes one gyrotron, a superconducting magnet and its refrigerator, and auxiliary power supplies for the gyrotron (such as the superconducting magnet power supply, ion pump power supply, collector coil power supply, and filament power supply).

For this expansion system, each gyrotron is equipped with an independent cathode high-voltage power supply and an independent anode high-voltage power supply. The megawatt-level high-power millimeter-wave generated by the gyrotron system is transmitted through the vacuum transmission lines to a quasi-optical antenna. This antenna couples the high-power millimeter-waves into the plasma to achieve plasma heating and current drive. The control and protection system manages the operational sequence of the system, monitors various real-time operational data, coordinates and commands all subsystems to operate orderly according to set parameters, and executes protective actions in case of system faults. The active cooling system is responsible for cooling all components within the system, including the gyrotron, the transmission lines, and the antenna.

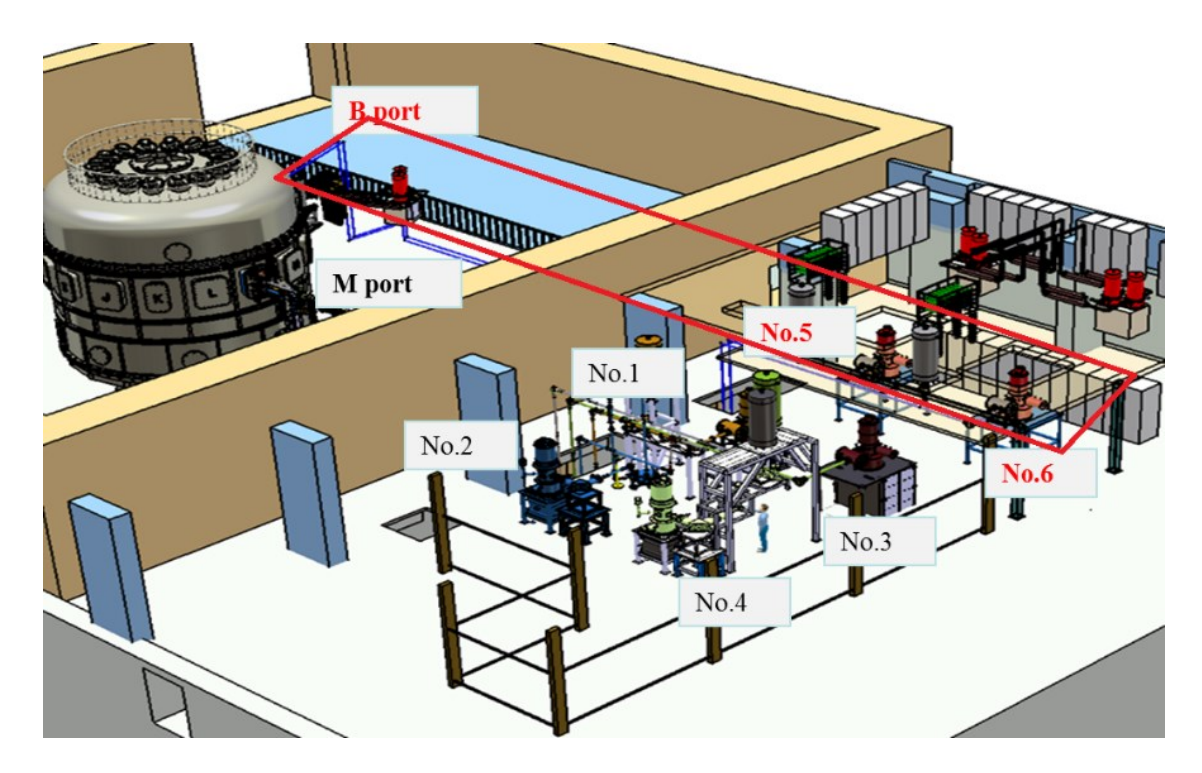


Fig. 1. The layout diagram of the EAST ECRH system, where the extended #5 and #6 systems are in the red rectangular area.

## 3. TRANSMISSION LINES AND ANTENNA

The corrugated circular waveguides are the main parts of the transmission lines for Phase I ECRH system. To maintain system compatibility, the upgraded #5 and #6 systems will also utilize this type of waveguide. The gyrotrons of the ECRH expansion system are located in Hall 8-1, with antennas positioned at the B port of the EAST device. The new #5 and #6 electron cyclotron transmission lines share the original 2.45GHz transmission line conduit (the original 2.45GHz transmission lines have been dismantled) with the upgraded 4.6GHz lower hybrid wave transmission lines. They connect the #8-1 gyrotron area to the antenna at Port B of EAST. Based on millimeter-wave transmission characteristics and the spatial constraints of the current channels, two parallel transmission lines were optimized. As shown in Fig. 2, each line undergoes 10 directional changes, and the combined total length of both lines is approximately 120 meters. Each transmission line has a power capacity of 1 MW and operates at frequencies of 140/105 GHz, meeting the requirements for continuous-wave operation. The layout in the tunnel-crossing area is shown in Fig. 3. Each transmission line is equipped with three sets of vacuum pumping systems, located near the MOU, the water load, and the CVD window on the antenna side, respectively.

The corrugated circular waveguide is a fundamental transmission component in ECRH systems. It is realized by grooving the inner wall of a conventional smooth circular waveguide. Its design structure is shown in Fig. 4 (a). The internal groove parameters of the corrugated circular waveguide are determined by its operating frequency. According to the microwave transmission characteristics of corrugated circular waveguides, when the depth of the internal grooves is an odd multiple of a quarter wavelength, the internal hybrid modes reach an equilibrium state, resulting in the lowest transmission loss. The groove period determines the internal harmonic ratio and the operating frequency band. Based on the above principles, the design parameters for the internal groove dimensions of the waveguide are as follows: period p = 0.65 mm, groove width p = 0.45 mm, and groove depth p = 0.45 mm.

The waveguide aperture parameter is determined by the required microwave power capacity it needs to transmit. According to the single-channel transmission power value of the EAST facility's ECRH system, the radius of the corrugated circular waveguide is selected to be a=31.75 mm. The waveguide material is aluminum alloy, chosen for its excellent mechanical properties, high strength, ease of processing, and relatively light weight, which facilitates alignment, installation, and debugging. Meanwhile, to ensure operational safety during prolonged microwave transmission, a water-cooled jacket is designed for the outer surface of the waveguide. The overall structure of the waveguide is shown in *Fig. 4* (b).

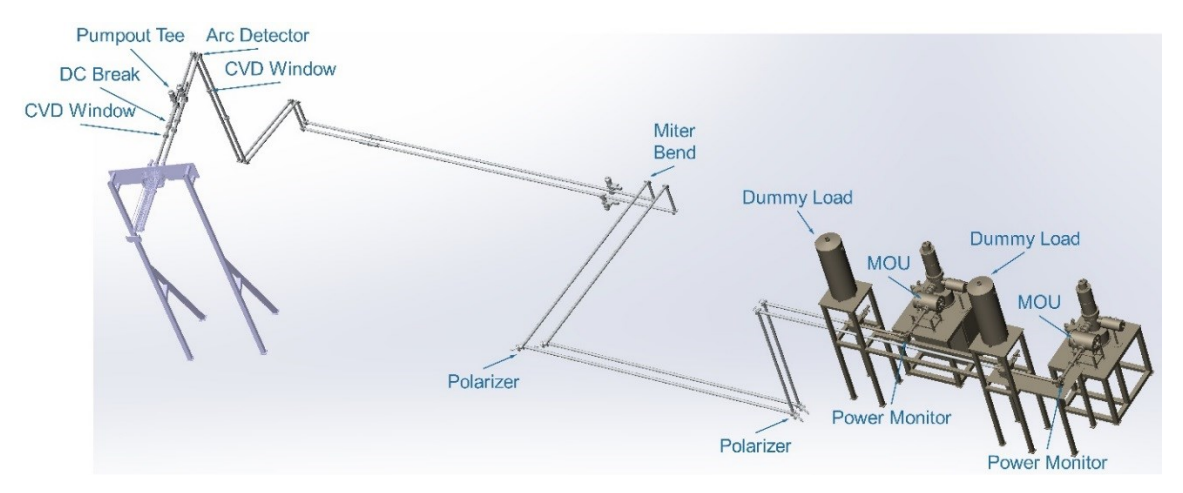


Fig. 2. The layout of the transmission lines for the electron cyclotron heating expansion system.

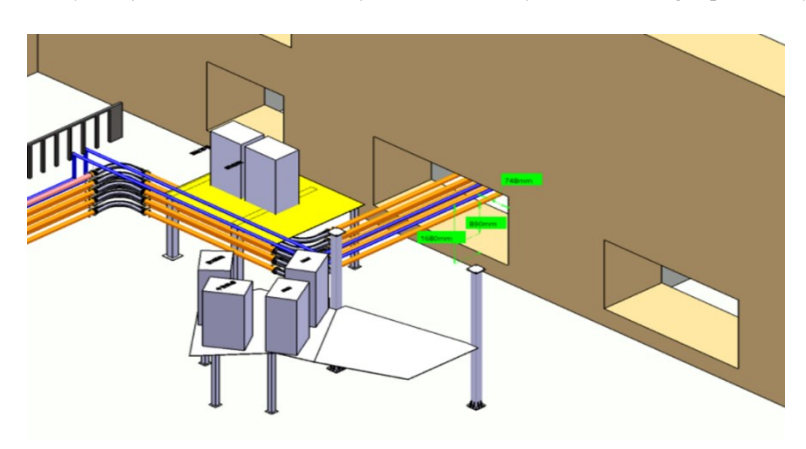


Fig. 3. The upgraded #5 and #6 electron cyclotron transmission lines (blue) share a common conduit with the lower hybrid wave transmission lines, passing through the service tunnel on the northeast side of the EAST hall.



Fig. 4. The structure (a) and the model (b) of the corrugated waveguide.

The antenna of the upgraded ECRH system shares horizontal Port B [2] with the upgraded 4.6GHz Lower Hybrid Wave (LHW) system. Port sharing reflects EAST's compact design, necessitating innovative integration of auxiliary heating systems. The antenna for the ECRH expansion system is shown in Fig. 5, which includes four parts: the quasi-optical transmission and emission unit, the internal support component, the shielding and protection unit, and the external support component.

The quasi-optical transmission and emission unit shown in *Fig.* 6 is the core component of the antenna. There are two independent transmission and emission units. Each unit utilizes two metal mirrors based on the quasi-optical characteristics of millimeter waves to achieve microwave power injection. Each unit consists of a 2.6-meter-long 63.5 mm stainless steel waveguide, a focusing mirror, and a rotating mirror with a drive mechanism. The stainless steel waveguide connects to the external transmission system of the antenna, enabling microwave feed into the antenna interior. The focusing mirror and rotating mirror form a quasi-optical emission mirror set, which constrains the beam characteristics and adjusts the emission angle to achieve precise microwave power deposition. The emission centers of the two beams are 350 mm apart from the central horizontal plane of EAST. The major radius R [6] of the emission point is 2750 mm, and the optimal current drive poloidal angle is 111°. The incident

distance of the focusing mirror is the distance from the waveguide port to the reflective center of the focusing mirror, denoted as  $z_1 = 240$  mm. The angle  $\theta$  between the incident beam and the reflected beam of the focusing mirror is 118.6°. The distance from the center of the focusing mirror to the center of the rotating mirror is  $z_2 = 125$  mm, and the distance from the center of the rotating mirror to the plasma resonance layer is  $z \approx 1200$  mm. To balance the conflict between minimizing the beam waist of the ECW within the plasma resonance layer and the engineering constraint that the focusing mirror size, optimization calculations yielded the following results: The ellipsoidal surface has a semi-major axis a = 1.311 m and a semi-minor axis a = 1.311 m and a semi-minor axis a = 1.311 m, as shown in Fig. 7.

When transmitting high-power millimeter waves, components such as the stainless steel waveguide, ellipsoidal focusing mirror, and rotating mirror will generate heat due to Ohmic losses and mode conversion losses. Therefore, they are all designed with active cooling functionality. Among these, the stainless steel input waveguide, with a total length of 2.6 meters, will be formed by connecting two 1.3-meter waveguides, one of which is equipped with a CF100 flange. The stainless steel waveguide employs a welded water jacket design, as illustrated in *Fig. 8*.

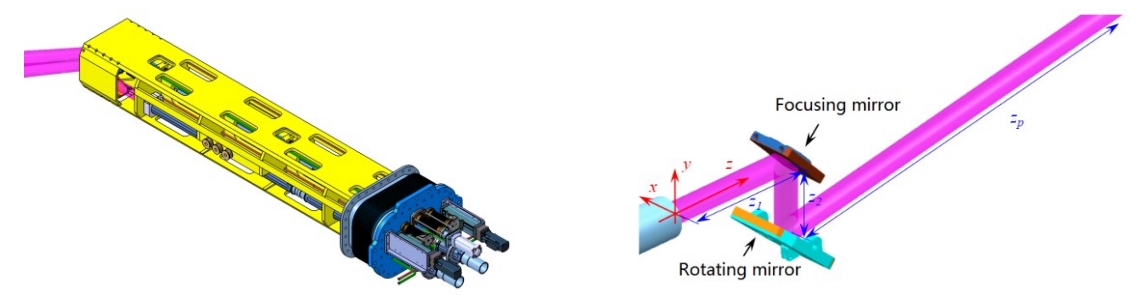


Fig. 5. The antenna for the electron cyclotron heating Fig. 6. The quasi-optical transmission and emission unit. expansion system.

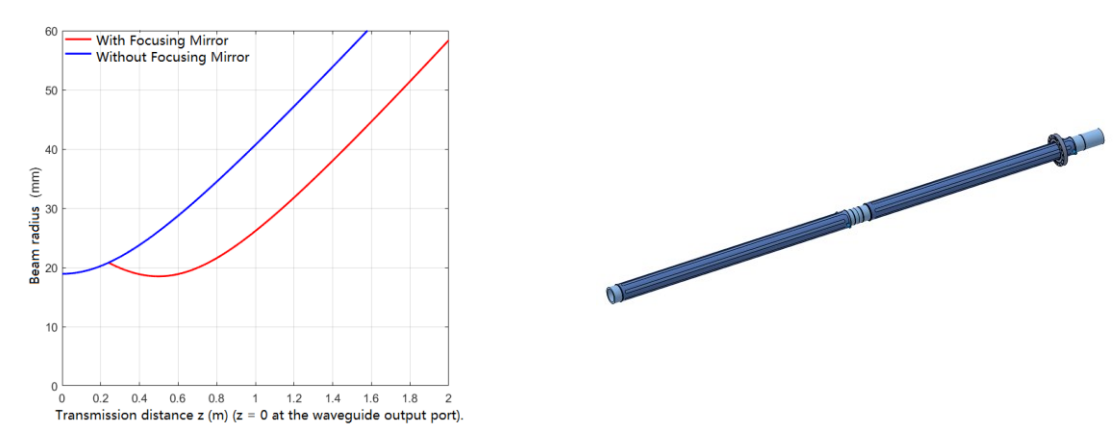


Fig. 7. The evolution of beam radius with transmission distance.

Fig. 8. The stainless steel waveguide.

Both the focusing mirror and the rotating mirror are constructed by welding a chromium zirconium copper reflector with a cooling channel design to stainless steel support cover plates. The focusing mirror measures 175 mm  $\times$  90 mm, with its water inlet and outlet located on the side of the mirror's wider edge. The rotating mirror measures 200 mm  $\times$  120 mm, with its water inlet and outlet situated on the stainless steel support plate. The rotating mirror employs a ball-joint connecting rod drive mechanism to achieve polar rotation control of the beam angle, as shown in *Fig.* 9. The rotation of the mirror is driven and controlled via a motor and a main shaft.



Fig. 9. The schematic of the focusing mirror (left) and the rotating mirror (with drive mechanism, right).

We conducted a multiphysics analysis on the emission mirrors. The runner structure, temperature distribution, stress distribution, and deformation distribution of the mirrors are detailed in Table 1. The flow rate is 0.125kg/s for the focusing mirror, and the flow rate is 0.196kg/s for the rotating mirror. The inlet temperature of the water is 35 °C. For the focusing mirror, only the microwave Ohmic loss was considered, while for the rotating mirror, both the microwave Ohmic loss and the plasma radiation heat were taken into account. The analysis results indicate that the design of the antenna emission mirror meets the requirements. We also performed a stress analysis on the antenna support assembly, which showed a maximum deformation of only 0.18 mm and an overall maximum stress of 26.3 MPa, confirming that it satisfies the demands. Due to space constraints, detailed descriptions are omitted here

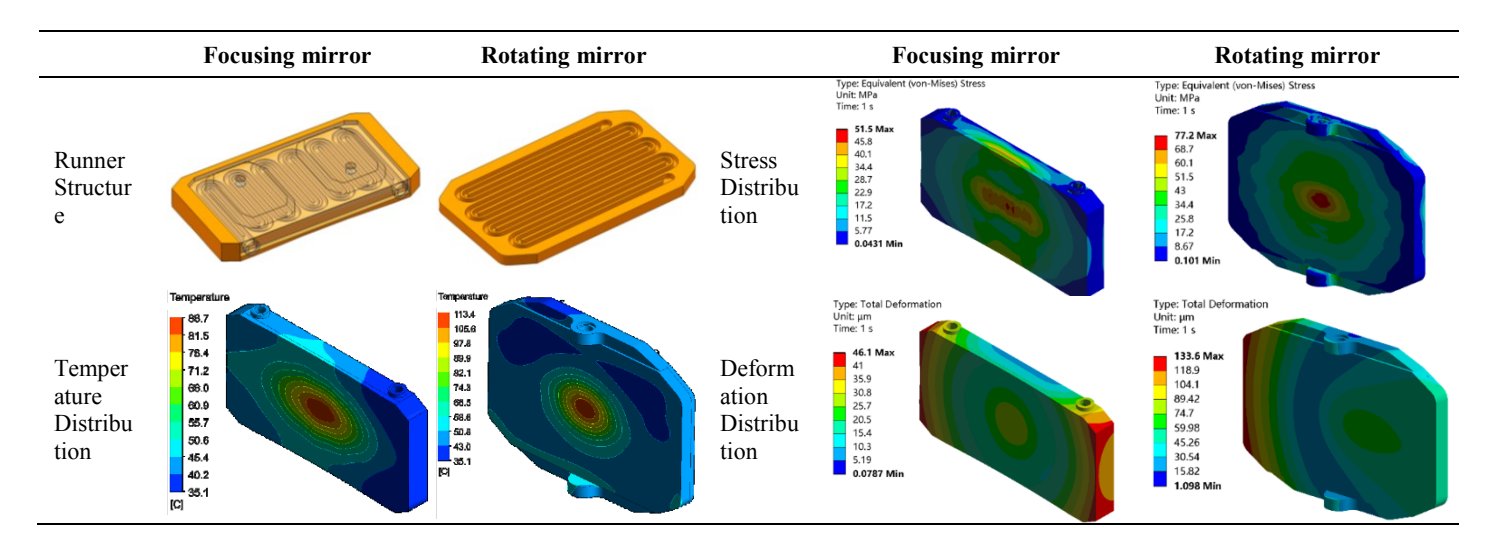


TABLE 1. RESULTS OF THE MULTIPHYSICS ANALYSIS ON THE EMISSION MIRRORS.

## 4. CONTROL SYSTEM

The independent control system for the #5 and #6 systems was designed, including a new automatic restart control system and a new real-time power control system. The real-time power control system is designed to receive power demand signals from the Plasma Control System (PCS) [7] and output the corresponding power to meet the more flexible power requirements of EAST experiments. A new central timing controller has been designed with three operating modes: system self-check mode, test mode, and EAST experiment mode. In test mode and EAST experiment mode, the automatic restart function can be enabled, allowing the gyrotron to restart automatically in the event of a fault interruption.

The proposed control system can be divided into the following eight parts: central timing control, interlock protection, overcurrent protection, arc protection, RF protection, data acquisition and power measurement, real-time power control, and video monitoring. All parts of the control system are independent of those in the Phase I ECRH system. For this expanded ECRH system, the central timing control system has been further optimized, particularly with the addition of an automatic restart function. The RF protection system uses a new independent cRIO-9049 device as the lower-level controller. Since the lower-level controller used in the Phase I ECRH RF protection system is a cRIO-9024 [8], we designed the system to use the same upper-level control software to manage both cRIO devices. For device compatibility, the upper-level control program will be developed in LabVIEW 2019 (32-bit) on the Windows 10 64-bit operating system. The data acquisition system uses a PXI-8842 device, operates independently of the Phase I ECRH data acquisition system, and the upper-level control program will be developed in LabVIEW 2024 (32-bit) on a Windows 10 64-bit system. The other parts of the control and protection systems are similar to those [9,10] in the first-phase ECRH system. In the following, we provide more details of the design of the subsystems that have undergone significant changes compared to the Phase I ECRH control system.

## 4.1. Central timing controllers

There are two central timing controllers in Phase II. One central timing controller corresponds to one gyrotron system. The new central timing controller has been designed for each gyrotron with three operating modes: system

self-check mode, gyrotron test mode, and EAST experiment mode. In test mode and EAST experiment mode, the automatic restart function can be enabled, allowing the gyrotron to restart automatically in the event of a fault interruption. That ensures rapid recovery of gyrotrons after transient faults to maintain plasma stability.

# 4.1.1. EAST experiment mode

Under the EAST experimental mode, the restart sequence is shown in *Fig. 10*. If the input signal in the figure changes to a low level prematurely, the system will immediately initiate a shutdown procedure. Depending on whether the auto-restart function is enabled, the system will decide whether to start up again.

The EAST central control PCS system sends three signals to the central timing controller: the Ip signal, the EAST ready signal, and the EAST trigger signal. The Ip signal is used to indicate the plasma current, with a high level indicating the presence of plasma current and a low level indicating the absence of plasma current. When the central control selects to use the ECRH system for plasma heating, the EAST ready signal can be activated high to the EC system 50s to 10s earlier; when the central control does not select the ECRH heating system, the EAST ready signal remains low. The EAST trigger signal is the trigger signal for ECRH, and its high-level state indicates the desired ECRH wave output state.

After receiving the protection summary signal, if only fast protection is active, the protection duration is 200ms. If it is still within the discharge pulse width, then after time t1 (300ms), an anode voltage reset signal is issued; after another t2 (0 or 100ms), a cathode voltage reset signal is issued; after another t3 (0 or 100ms), a reset signal for the GYCOM arc protector is issued; and after another t4 (200ms), triggering begins.

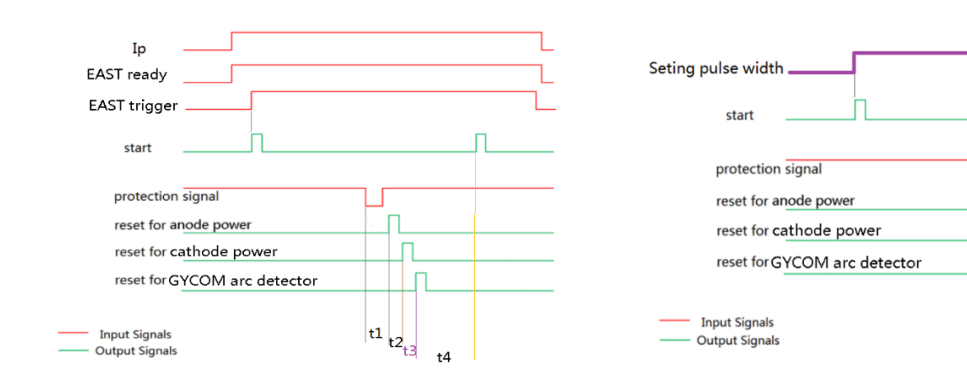


Fig. 10. The automatic restart logic and timing for ECRH expansion system under the EAST experimental mode.

Fig. 11. The automatic restart logic and timing for ECRH expansion system under gyrotron test mode.

## 4.1.2. Gyrotron test mode

The operating sequence for restart in the gyrotron test mode is shown in *Fig. 11*. Timing begins after the start trigger. If the input signal (protection signal) changes to a low level before the pulse width is completed, the system will immediately initiate a shutdown procedure. If the auto-restart function is enabled, an automatic restart will be initiated. Note that the total pulse width remains unchanged. After the cumulative wait time and wave-output time from multiple triggers reach the total pulse width, a stop signal is issued.

As with the EAST experimental mode, after receiving the protection signal, if only fast protection is active, the protection duration is 200 ms. If it is still within the discharge pulse width, then after time t1 (300 ms), an anode voltage reset signal is issued; after another t2 (0 or 100 ms), a cathode voltage reset signal is issued; after another t3 (0 or 100 ms), a reset signal for the GYCOM arc protector is issued; and after another t4 (200 ms), triggering begins.

# 4.2. RF protection system

The RF protection system is used for high-reflection protection and no-wave protection (dropping out of the RF generation mode with normal high voltages), and it enables real-time monitoring of the gyrotron's output power [8]. Since significant deviations in the waveguide transmission system alignment can lead to excessively high reflected power, it is necessary to establish high-reflection protection to ensure system safety. When the gyrotron

enters a competition mode, resulting in no wave output, the high voltage must be immediately cut off to protect the gyrotron. Among these, the no-wave protection is always active. The logic for high-reflection protection is as shown in Table 2. It only takes effect when both the cathode and anode voltages are powered on simultaneously. This design prevents false triggers of high-reflection protection due to other interfering factors when the gyrotron is not generating waves.

TABLE 2. HIGH-REFLECTION PROTECTION LOGIC

Reflected Voltage > Threshold	Anode Voltage Present	Cathode Voltage Present	Output
1	1	1	0
0	1	1	1
X	0	1	1
X	1	0	1
X	0	0	1

Note: "X" denotes a "don't care" condition, meaning the output depends solely on the anode and cathode voltage states in these cases.

The RF protection system uses a new independent cRIO-9049 device as the lower-level controller. Four synchronous analog input modules (NI 9223), two analog output modules (NI 9269), and two digital I/O modules (NI 9401) will be used for RF signal data acquisition and protection signal output.

The analog input module NI-9223 is used to acquire the real-time RF power signals. The NI 9401 digital I/O module has two primary functions: firstly, it outputs protection signals to the central timing controller; secondly, it performs logical operations on digital signals. The central timing controllers output different start/stop trigger signals for two sets of gyrotrons. The OR operation of the two start/stop signals can be implemented in hardware utilizing the FPGA of the cRIO and the NI 9401 digital I/O. The resulting signal is then sent to the PXI for hardware triggering for data acquisition, enabling one data acquisition system to acquire the data of two sets of independently controlled gyrotrons.

For the convenience of the RF protection system operation, we plan to use the same upper-level control software to manage both cRIO devices for Phase I and Phase II. Since the lower-level controller used in the Phase I ECRH RF protection system is a cRIO-9024, for device compatibility, the upper-level control program will be developed in LabVIEW 2019 (32-bit) on the Windows 10 64-bit operating system. The architecture diagram of the RF protection system is shown in *Fig. 12*. The isolator is used to isolate the RF protection system from the central timing controllers. It converts the electrical signal output by the cRIO into an optical signal through electro-optical conversion. The optical signal is then transmitted via optical fiber, before being converted back into an electrical signal for transmission to the central timing controller.

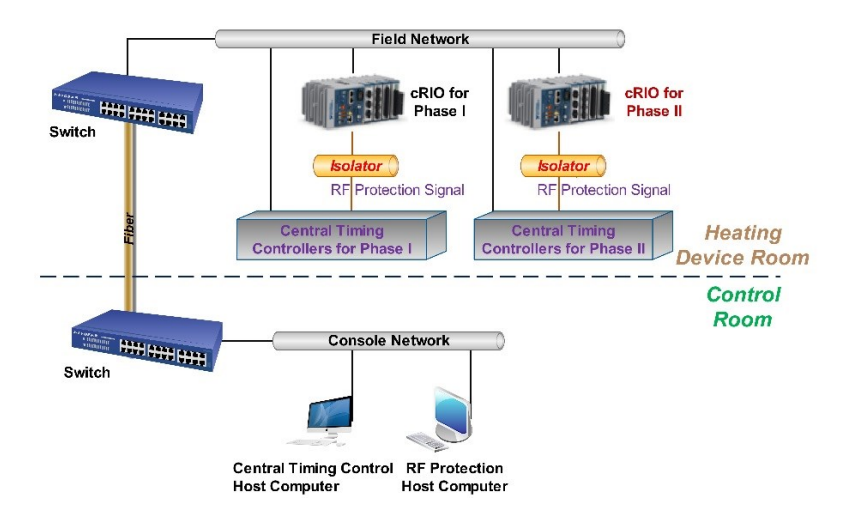


Fig. 12. The architecture diagram of the RF protection system (including both Phase I and Phase II).

#### 4.3. Real-time power control system

The real-time power control system is used to achieve real-time control of the gyrotron's output power during experiments. It receives power demand signals from the PCS for EAST and outputs the corresponding power to meet the more flexible power requirements of EAST experiments. The hardware architecture of the real-time power control system is shown in *Fig. 13*. It consists of an upper computer and a lower controller. The lower real-time controller interacts with the central timing controller, PCS, and high-voltage power supply through analog and digital input/output modules. The real-time power control program adopts a three-tier architecture. The top-level program runs on the Windows 11 system, the middle layer runs on a Linux real-time system, and the bottom layer is implemented based on FPGA.

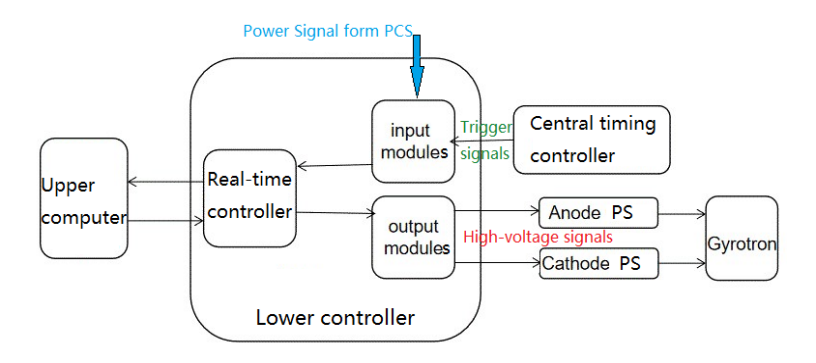


Fig. 13. The architecture diagram of the real-time power control system for ECRH expansion system.

#### 5. CONCLUSIONS

The expansion design enhances power delivery and frequency modulation to optimize energy deposition into the plasma, addressing challenges such as plasma turbulence and edge-localized modes (ELMs). As part of EAST's advanced heating and current drive (H&CD) systems, the ECH system plays a pivotal role in plasma heating and instability control. Its design focuses on extending operational capabilities to support long-pulse, high-performance plasma experiments, aligning with EAST's goal of steady-state nuclear fusion. To accommodate the entire operational range of EAST's toroidal field, the two additional systems, #5 and #6 systems, will primarily operate at 140 GHz but can switch to a secondary frequency of 105 GHz to adapt to EAST's low toroidal field operations. The ECRH expansion system will upgrade the four ECRH systems to six, enhancing ECRH's power output capability at the 140 GHz frequency point to 4.5 MW for up to 1000 seconds. The independent control system for the #5 and #6 systems was designed, including a new automatic restart control system and a real-time power control system.

### **ACKNOWLEDGEMENTS**

This work was supported in part by the National Natural Science Foundation of China under Grant 12405270; in part by the Upgrade and renovation of superconducting Tokomak Nuclear Fusion experimental device No. 2406-000000-04-02-630302.

# REFERENCES

- [1] Y. Song *et al.*, Ieee T Plasma Sci **50**, 4330 (2022).
- [2] W. Xu *et al.*, Ieee T Plasma Sci **52**, 5159 (2024).
- [3] Y. Song *et al.*, Science Advances 9, eabq5273 (2023).
- [4] J. Li, Y. Wan, and t. E. team, Engineering 7, 1523 (2021).
- [5] X. Gong, Nucl Fusion (2024).
- [6] M. H. Li et al., Nucl Fusion 65, 076017 (2025).
- [7] Q. P. Yuan *et al.*, Fusion Eng Des **129**, 109 (2018).
- [8] W. Xu, H. Xu, F. Liu, Y. Tang, Z. Wu, X. Wang, J. Wang, and J. Feng, IEEE Access 4, 5809 (2016).
- [9] W. Xu, H. Xu, F. Liu, H. Hu, and J. Feng, Ieee T Plasma Sci 47, 1887 (2019).
- [10] W. Xu, H. Xu, J. Feng, Y. Yang, H. Hu, F. Liu, and Y. Tang, IET Science, Measurement & Technology 12, 726 (2018).